SPE 80922

A New Robust Model For Natural Separation Efficiency

R.A. Marquez, SPE and M.G. Prado, SPE, University of Tulsa

This paper was prepared for presentation at the SPE Production and Operations Symposium held in Oklahoma City, Oklahoma, U.S.A., 22–25 March 2003.

Abstract

This paper presents a mechanistic model to predict natural separation efficiency. Based on drift-flux model, a new mathematical formulation was developed to estimate natural separation efficiency. The new model considers the existence of the slip velocity not only in the vertical direction, but also in the radial direction. The new and robust model is a function of important variables such as geometric characteristics of the bottomhole, slip velocity at both vertical and radial direction and the gas and liquid flow rates. Available experimental data was used to obtain a new correlation for the bubble drag radius, as a function of gas flow rate. Predictions of the model have been compared and verified against experimental data, showing good agreement.

Introduction

In the bottomhole a natural process occurs where gas associate to the oil is coming out of solution due to decreasing bottomhole flowing pressure below the bubble point. The presence of this free gas affects the production of a well, especially if this well is using any pumping system, since liquid drag part of this gas into the pump. Predicting how much free gas goes into the pump is a very important aspect for designing pumping systems.

Tulsa University Artificial Lift Projects TUALP has been conducting important researches in the area of natural separation since 1993. It has permitted design and built important experimental facilities in order to gather data on natural separation. In addition, some models have been developed as well, such as Alhanati (1993), Serrano (1999) and Harun (2000).

Analysis of those models showed that the accuracy in the prediction of natural separation efficiency depends not only on the treatment of the governing equations, but also on the assumptions considered in the solution of the problem. Although models have captured part of the physics involve in the process, their extension for all operational conditions has been limited. One reason could be related to the simplifying assumptions assumed. For example, Alhanati and Serrano's model never considered the effect of slip velocity in the radial direction, because neither a correlation nor a model was available for it.

Preliminary results obtained by Marquez and Prado (2003) showed how the slip velocity in the vertical and radial direction has an important effect in the prediction of natural separation efficiency. Marquez and Prado proposed a new model, which considers the slip velocity effect through a correlation obtained by fitting the model to available experimental data.

Because correlations do not work very well for all operational conditions, a new mechanistic model is proposed in this paper. Based on streamlines, an equation for the liquid phase velocity as a function of geometric characteristics of the bottomhole was determined. In addition, using the slip velocity definition with along the liquid velocity, the trajectory of a single bubble can be determined. The prediction of natural separation efficiency would be given as a geometric function of the trajectory of this bubble.

Literature Review

Alhanati (1993) designed and built an experimental facility to gather data about natural separation efficiency. Tests were performed in a full-scale experimental facility for three liquid levels (300, 600 and 900 bpd), two pressure levels (100 and 200 psig) and three levels of GLR (50, 100 and 200 scf/stb), using water and air as experimental fluids. Based on the drift-flux model, Alhanati (1993) developed the first simplified model to predict natural separation efficiency, assuming no slip velocity in the radial direction. This model showed good agreement with the available experimental data.

In 1999, Serrano expanded the Alhanati's test program. Experiments were carried out at different pressures (50, 100 and 150 psig). Three liquid flow rates (1000, 1500 and 2000 bpd) were considered. The gas flow rate varied from 2000 to 20000 scf/d. Air-water mixture was used as the test fluid. Also three different inclinations from horizontal were chosen (90, 60, and 30 degrees). Using this new experimental data, Serrano found that Alhnati's model failed to match this data. As a result, Serrano proposed a new simplified model based on the Alhanati's model, but assuming the existence of a different gas void fraction for the region in front of the pump intake.

No slip velocity in the radial direction was considered in this model as well. Experimental data was used to find a correlation between the gas void fraction of the fluids across the annulus and the gas void fraction of the fluid going into the pump. Limitations were found in the Serrano's model because cannot be used to gas void fraction greater than 20%.

Harun (2000) proposed a mechanistic model based on the combined phase momentum equation and a general slip closure relationship, applied to a single control volume situated in front of the pump intake. The solution of the system of equations may result complex and according to Harun, natural separation process can be described without considering the flow phenomenon occurring in the intake port direction.

Marquez and Prado (2003) presented a new simplified model to predict natural separation efficiency, based on the drift-flux model approach. The model considers the effect of the slip velocity in the radial direction, variable neglected in previous simplified models. In adittion, a correlation for this effect was obtained. Good agreement of this model with the experimental data showed the important effect that the slip velocity in the radial direction has in the prediction of natural separation.

General Formulation of the New Simplified Model

The new simplified model proposed in this research considers the existence of the slip velocity in the radial direction. Let's consider a single control volume in front of the pump intake, as shown in Fig. 1. There, three assumptions are assumed valid in this new modeling on natural separation efficiency. The first assumption states constant gas void fraction α_g across to the annulus domain and up to the pump intake port. The second assumption considers that the liquid column in the annulus in front and above the pump intake is not flowing in the vertical direction. The third assumption considers the existence of slip velocity between gas and liquid in the vertical and radial direction.

Assuming constant density, mass balance equation permits establishing a volumetric balance for each phase around the single control volume in front of the pump intake, as shown in Fig. 2.

Based on the volumetric balance for the gas phase, natural separation efficiency E, defined as the ratio of the gas flow rate vented Q_{gv} to the gas flow rate coming from the annulus Q_g^i, would be given by

$$E = \frac{Q_{gv}}{Q_g^i} = 1 - \frac{Q_{gp}^p}{Q_g^i} \qquad (1)$$

Q_{gp}^p represents the gas flow rate going into the pump. Gas flow rate can also be expressed as a function of superficial velocity and flow area, i.e.

$$\begin{aligned} Q_{gp}^p &= V_{rsg}^p \; A_p \\ Q_g^i &= V_{zsg}^i \; A_{Ann} \end{aligned} \qquad (2)$$

V_{rsg}^p and V_{zsg}^i represent the superficial gas velocity going into the pump and the superficial gas velocity coming from the annulus, respectively. A_p and A_{Ann} are the area of the port and the annulus, respectively, as a shown in Fig. 1. Combining Eqs. 1 and 2, natural separation efficiency would be given by

$$E = 1 - \frac{V_{rsg}^p}{V_{zsg}^i}\left(\frac{A_p}{A_{Ann}}\right) \qquad (3)$$

The ability to solve Eq. 3 depends basically on the facility to determine how much gas is going into the pump, i.e. V_{rsg}^p.

Based on the drift-flux model proposed by Ishii (1975) and assuming slip velocity in both directions, V_{rsg}^p and gas void fraction α_g can be obtained by

$$V_{rsg}^p = \frac{\alpha_g}{1-\alpha_g}\left[V_{r\infty} + V_{zsl}^i\left(\frac{A_{Ann}}{A_p}\right)\right] \qquad (4)$$

$$\frac{\alpha_g}{1-\alpha_g} = \frac{V_{zsg}^i}{V_{z\infty}} \qquad (5)$$

Details about the algebraic equations for V_{rsg}^p and α_g are shown in Appendix A. From Eqs. 3, 4 and 5, natural separation efficiency would be finally given by

$$E = 1 - \left[\left(\frac{V_{r\infty}}{V_{z\infty}}\right)\left(\frac{A_p}{A_{Ann}}\right) + \frac{V_{zsl}^i}{V_{z\infty}}\right] \qquad (6)$$

According to Eq. 6, natural separation efficiency depends on superficial liquid velocity V_{zsl}^i, geometric configuration of the bottomhole A_p / A_{Ann}, and the terminal velocity ratio $V_{r\infty} / V_{z\infty}$.

All variables can be easily determined, except $V_{r\infty}$ because no modeling is available for this variable. Therefore, it will represent the biggest unknown variable of this simplified model. In this study, a model will be considered as a solution of $V_{r\infty}$.

Sip Velocity Analysis

Mass and momentum balance equations will allow to obtaining an analytical solution for slip velocity at r and z direction, assuming the following considerations.

1. Steady state (no transient effects)
2. Both the average pressure and stress in the bulk fluid and the interface are approximately the same
3. No mass transfer
4. Density and viscosity are constant
5. 2-dimensional, cylindrical coordinate (r , z)
6. Axis-symmetric
7. Viscous and friction effects are negligible
8. The gas phase (k=g) is dispersed in a continuous liquid phase (k=l)

Mass and momentum balance equation can be written as
Mass Balance Equation:

$$\frac{1}{r}\frac{\partial}{\partial r}(\alpha_k\ \rho_k\ r\ V_{rk}) + \frac{\partial}{\partial z}(\alpha_k\ \rho_k\ V_{zk}) = 0 \qquad (7)$$

Momentum Balance Equation at the radial direction:

$$V_{rk}\frac{\partial}{\partial r}(\alpha_k\ \rho_k\ V_{rk}) + V_{zk}\frac{\partial}{\partial z}(\alpha_k\ \rho_k\ V_{rk}) = -\alpha_k\frac{\partial}{\partial r}(P_k) + \vec{M}_k \qquad (8)$$

Momentum Balance Equation at the vertical direction:

$$V_{rk}\frac{\partial}{\partial r}(\alpha_k\ \rho_k\ V_{zk}) + V_{zk}\frac{\partial}{\partial z}(\alpha_k\ \rho_k\ V_{zk}) = -\alpha_k\frac{\partial}{\partial z}(P_k) + \alpha_k\ \rho_k\ \vec{g} + \vec{M}_k \qquad (9)$$

Sip Velocity in the Vertical Direction.
Let's consider a multi-particle system in an infinite medium under the condition that liquid and gas bubble are moving in the vertical direction, only.
The solution of mass and momentum balance equations, with along the interfacial drag force definition, would allow to obtain the following equation for the slip velocity in the vertical direction V_{zs}.

$$V_{zs}\ \frac{8\,r_d}{a_i\ r_{sm}\ C_d\ |\vec{V}_s|}\ \alpha_g\ (1-\alpha_g)\frac{(\rho_l-\rho_g)\,g}{\rho_l} \qquad (10)$$

According to Eq. 10, V_{zs} is a function of the bubble shape, gas void fraction α_g, fluids density, and drag coefficient C_d. Details about this algebraic equation have been included in Appendix B.

Sip Velocity in the Radial Direction.
Similar to the vertical direction, let's consider a multi-particle system in an infinite medium under the same conditions, but assuming that the liquid and gas bubble are moving only in the radial direction. The slip velocity in the radial direction V_{rs} would be given by

$$V_{rs} = \frac{8\,r_d}{a_i\ r_{sm}\ C_d\ |\vec{V}_s|}\ \alpha_g\ (1-\alpha_g)\left(V_{rl}\ \frac{d}{dr}(V_{rl})\right) \qquad (11)$$

Appendix C shows the algebraic formulation of V_{rs}. On the other hand and according to Eq. 11, the slip velocity in the radial direction V_{rs} shows a strong dependence on how fast the liquid phase accelerates into the pump.

Sip Velocity Ratio.
According to Eqs. 10 and 11, the slip velocity in the radial and vertical direction are given by

$$V_{rs} = \frac{8\,r_d}{a_i\ r_{sm}\ C_d\ |\vec{V}_s|}\ \alpha_g\ (1-\alpha_g)\left(V_{rl}\ \frac{d}{dr}(V_{rl})\right)$$

$$V_{zs} = \frac{8\,r_d}{a_i\ r_{sm}\ C_d\ |\vec{V}_s|}\ \alpha_g\ (1-\alpha_g)\frac{(\rho_l-\rho_g)\,g}{\rho_l}$$

Dividing both solutions, the following relationship can be obtained

$$\frac{V_{rs}}{V_{zs}} = \frac{\rho_l}{(\rho_l-\rho_g)\,g}\left(V_{rl}\ \frac{d}{dr}(V_{rl})\right) \qquad (12)$$

On the other hand, the drift-flux model proposed by Ishii (1975) can be used to obtaining an auxiliary expression, which relates the slip velocity with the terminal velocity at any direction. Those equations are given by

$$V_{rs} = V_{r\infty}\ (1-\alpha_g)^{n-1}$$

$$V_{zs} = V_{z\infty}\ (1-\alpha_g)^{n-1}$$

Dividing both definitions, the following ratio would result valid

$$\frac{V_{rs}}{V_{zs}} = \frac{V_{r\infty}}{V_{z\infty}} \qquad (13)$$

Therefore, the relative terminal velocity $V_{r\infty}/V_{z\infty}$ would be given by

$$\frac{V_{r\infty}}{V_{z\infty}} = \frac{\rho_l}{(\rho_l-\rho_g)\,g}\left(V_{rl}\ \frac{d}{dr}(V_{rl})\right) \qquad (14)$$

The analytical solution of Eq. 14 is not easy when a macroscopic analysis on just one cell is considered. However, its qualitative analysis show that the terminal velocity ratio is proportional to how fast the liquid is moving from the annulus to the pump intake.

Natural separation efficiency would be given finally by

$$E = 1 - \left[\left(\frac{V_{r\infty}}{V_{z\infty}}\right)\left(\frac{A_p}{A_{Ann}}\right) + \frac{V_{zsl}^{i}}{V_{z\infty}}\right]$$

Where

$$\frac{V_{r\infty}}{V_{z\infty}} = \frac{\rho_l}{(\rho_l-\rho_g)\,g}\left(V_{rl}\ \frac{d}{dr}(V_{rl})\right)$$

Modeling on the Streamlines

Liquid-Phase Velocity.
Let's consider that a liquid phase only is coming from the annulus and going into the pump only, under the following assumptions:

1. Steady state condition
2. Density and viscosity constant
3. Constant velocity profile at the inlet
4. The liquid is considered stagnant above the port of the intake pump
5. Axis-symmetric

Based on the geometric characteristics of the bottomhole, as shown in Fig. 4, mass balance equation would allow to obtain the following equation for the liquid phase velocity in the horizontal direction V_{rl} as a function of any r and h_i

$$V_{rl} = \left(\frac{r_p}{r} + \frac{h_i}{h_p} \frac{(r_c - r_p)}{r} \right) V_{zl}^i \; Tan\beta \qquad (15)$$

Eq. 15 represents the liquid phase velocity profile at the radial direction V_{rl}. This equation represents a big step in the prediction of natural separation efficiency because the model is sensible to geometric characteristics of the bottomhole such as annulus and port size. Fig. 5 shows how this velocity profile change with r and h_i.

Gas-Phase Velocity.
Now, consider that a single bubble of gas goes into the pump and it is desired to know the velocity of this bubble at both radial and vertical direction.

For it, a force balance around a single gas bubble at the vertical direction can be considered. According to Fig. 6, that force balance would be given by

$$\vec{F}_d + \vec{F}_p + \vec{F}_g = 0 \qquad (16)$$

Where,

$$F_d = \frac{1}{2} C_d \; \rho_l \; A_d \; V_{zs} \left| \vec{V}_s \right| \qquad (17)$$

$$F_p = B_d \; \vec{\nabla} P = B_d \; \frac{dP}{dz} \qquad (18)$$

$$F_g = B_d \; \rho_g \; g \qquad (19)$$

Solving Eq. 16, the slip velocity in the vertical direction V_{zs} would be defined by

$$V_{zs} = \frac{8}{3} \frac{r_d}{C_d \left| \vec{V}_s \right|} \frac{(\rho_l - \rho_g)\, g}{\rho_l} \qquad (20)$$

Since the liquid in front of the pump intake is moving in the radial direction only, the slip velocity definition would allow to obtain one expression for the gas-phase velocity in the vertical direction V_{zg}, which would be given by

$$V_{zs} = V_{zg} \qquad (21)$$

Combining Eqs. 20 and 21, the gas phase velocity in the vertical direction V_{zg} would be finally given by

$$V_{zg} = \frac{2}{9} \frac{r_d}{C_d \left| \vec{V}_s \right|} \frac{(\rho_l - \rho_g)\, g}{\rho_l} \qquad (22)$$

According to Fig. 7, In the radial direction a force balance around the gas bubble would permit to obtain the following equation.

$$\vec{F}_d + \vec{F}_p = 0 \qquad (23)$$

Where,

$$F_d = \frac{1}{2} C_d \; \rho_l \; A_d \; V_{rs} \left| \vec{V}_s \right| \qquad (24)$$

$$F_p = B_d \; \vec{\nabla} P \qquad (25)$$

Solving Eq. 23, the slip velocity in the radial direction V_{rs} may be defined as a function of liquid velocity V_{rl} by

$$V_{rs} = -\frac{8}{3} \frac{r_d}{C_d \left| \vec{V}_s \right|} V_{rl} \frac{d}{dr}(V_{rl}) \qquad (26)$$

V_{rs} depends on how fast the liquid-phase goes into the pump. The solution of this equation will require of an expression for the liquid velocity, which would be given by Eq. 15, and its derivative respect to r. This derivative is given by the following equation.

$$\frac{dV_{rl}}{dr} = -\left(\frac{r_p}{r^2} + \frac{h_i}{h_p} \frac{(r_c - r_p)}{r^2} \right) V_{zl}^i \; Tan\beta \qquad (27)$$

Replacing Eqs. 15 and 27 into Eq.26, the slip velocity in the radial direction V_{rs} would be defined by

$$V_{rs} = \frac{8}{3} \frac{r_d}{C_d \left| \vec{V}_s \right|} \frac{1}{r^3} \left[\left(r_p + \frac{h_i}{h_p}(r_c - r_p) \right) V_{zl}^i \; Tan\beta \right]^2 \qquad (28)$$

Finally, the slip velocity definition can be used, so the gas phase velocity in the radial direction V_{rg} would be given by

$$V_{rg} = \left(r_p + \frac{h_i}{h_p}(r_c - r_p) \right) V_{zl}^i \; Tan\beta \left[\frac{8}{3} \frac{r_d}{C_d \left| \vec{V}_s \right|} \frac{1}{r^3} \left(r_p + \frac{h_i}{h_p}(r_c - r_p) \right) V_{zl}^i \; Tan\beta + \frac{1}{r} \right] \qquad (29)$$

Trajectory of a Single Bubble.
Using definition, the velocity of the gas bubbles in the vertical and radial direction are given by

$$V_{zg} = \frac{dz}{dt}$$

$$V_{rg} = \frac{dr}{dt}$$

Assuming constant dt, the position of any bubble in the vertical and radial direction may be determined by

$$\frac{dr}{dz} = \frac{V_{rg}}{V_{zg}} \qquad (30)$$

Or simply

$$\frac{dr}{dz} = \frac{9}{2} \frac{C_d \left| \vec{V}_s \right|}{r_d} \frac{\rho_l}{(\rho_l - \rho_g)\, g} \left(r_p + \frac{h_i}{h_p}(r_c - r_p) \right) V_{zl}^i \; Tan\beta \left[\frac{8}{3} \frac{r_d}{C_d \left| \vec{V}_s \right|} \frac{1}{r^3} \left(r_p + \frac{h_i}{h_p}(r_c - r_p) \right) V_{zl}^i \; Tan\beta + \frac{1}{r} \right] \qquad (31)$$

The solution of Eq. 31 will allow to determine the position of a single bubble into the cell domain.

Assuming Stokes flow, .the drag coefficient C_d and the particle Reynolds Number Re_p are given by

$$C_d = \frac{24}{\mathrm{Re}} \quad (32)$$

$$\mathrm{Re}_p = \frac{2\, r_d \left|\vec{V}_s\right| \rho_l}{\mu_l} \quad (33)$$

Combining Eqs. 32 and 33 and replacing into Eq. 31, the differential equation would be finally given by

$$\frac{dr}{dz} = 54 \frac{\mu_l}{r_d^2} \frac{1}{(\rho_l - \rho_g)\, g} \left(r_p + \frac{h_i}{h_p}(r_c - r_p) \right) V_{zl}^i \, Tan\beta \quad (34)$$
$$\left[\frac{2}{9} \frac{r_d^2\, \rho_l}{\mu_l} \frac{1}{r^3} \left(r_p + \frac{h_i}{h_p}(r_c - r_p) \right) V_{zl}^i \, Tan\beta + \frac{1}{r} \right]$$

The position of a bubble into the annulus domain can be estimated by solving numerically the differential equation given by Eq. 34.

The position will be tracked into the flow domain until the bubble hit a certain position of the annulus domain, as shown in Fig. 8. If a bubble finally hit the upper section of the pump intake, see Fig. 8, it would be considered vented through the annulus. Otherwise, the bubble is considered dragged by the pump. It is valid assume that under any operational condition, there must be a point at the annulus inlet, at which the bubble stars and finally hit the upper side of the pump intake. As shown in Fig. 9, this point is corresponding to an imaginary circle called separation circle. Natural separation efficiency would be determined how the fraction of the cross sectional area beyond of the separation circle to the total cross sectional area of the annulus.

Closure Relationship for Drag Radius.
The solution of Eq. 34 requires also of an additional equation for drag radius. Using available experimental data in TUALP with along Eq. 34, several values for bubble drag radius r_d were determined. Those values were used to calculate the interfacial area concentration a_i. Definition used to determine the volumetric concentration of the interfacial area, in bubbles with any shapes. a_i is given by

$$a_i = \frac{3\,\alpha_g}{r_d} \quad (35)$$

Where α_g can be obtained from Eq. 5. On the other hand, a plot of interfacial area concentration a_i vs. superficial gas velocity has been obtained, as shown in Fig. 10. Good trend of the curve can be observed in that figure, so a new correlation was obtained for a_i as a function of the superficial gas velocity coming from the annulus V_{zsg}^i.

The new correlation for the interfacial area concentration a_i is given by

$$a_i = 5660.705\,(1 - e^{-2.5483248\, V_{zsg}^i}) \quad (36)$$

Therefore, the following equation for the bubble drag radius r_d would be given by

$$r_d = \frac{3}{5660.705\,(1 - e^{-2.5483248\, V_{zsg}^i})} \frac{V_{zsg}^i}{(V_{zsg}^i + V_{z\infty})} \quad (37)$$

According to Eq. 37, the bubble drag radius r_d depends on how much gas is coming from the annulus, i.e. V_{zsg}^i; variable extremely important in the modeling on natural separation efficiency and which had never been considered in previous simplified models.

Eq. 37 was used to solve the differential equation given by Eq. 34. Using available experimental data, a graph of Measured vs. Predicted Efficiency has been plotted, as shown in in Fig.11. Good agreement of the model with the experimental data was obtained.

VII. Analysis and Results

Model Comparisons.
The evaluation of this study was based on statistical parameters given by average percentage error $E1$, absolute average percentage error $E2$ and the standard deviation $E3$.

$$E1 = \left(\frac{1}{N} \sum_{i=1}^{N} e_{ri} \right) 100 \quad (54)$$

$$E2 = \left(\frac{1}{N} \sum_{i=1}^{N} \left| e_{ri} \right| \right) 100 \quad (55)$$

$$E3 = \sqrt{ \left(\frac{1}{N-1} \sum_{i=1}^{N} \left(e_{ri} - \frac{E1}{100} \right)^2 \right) }\; 100 \quad (56)$$

N represents the number of data points. The error e_{ri} is given by

$$e_{ri} = \frac{E_{cal,i} - E_{meas,i}}{E_{meas,i}} \quad (57)$$

The performance of the new mechanistic model proposed in this paper can be compared with another simplified models by using the percentage error equations shown previously. Results are shown in Table 1.

According to Table 1, the new mechanistic model performs better than previous simplified models. The overall performance of Ahlanati's model represents a 25.64 % against of 15.24 % of the new simplified model proposed.

Effect of Geometry.
Geometric characteristics of the bottomhole are considered in this mechanistics model. The model allowed setting the port and the annulus size.

As reported by Ghauri (1979), casing size is an important factor in submersible pump performance. The larger is annulus area; the better is natural separation efficiency. The new mechanistic model was used to predict natural separation efficiency for a 4 in. outside pump diameter inside 5, 6.366

and 10 in. casings. According to Fig. 12, natural separation increases as the annulus area increases.

Port size is another variable considered by this model. Fig. 13 shows the effect of this variable on natural separation process. According to this figure, the bigger is the port size; the bigger is natural separation efficiency. Those results make sense when the acceleration of the fluids is considered. The bigger is the acceleration of the fluids going into the pump; the lower is the natural separation efficiency. This phenomenon would occur for smaller port sizes. Because no experimentals results are available about this effect, the analysis in depth and the comparisons of these results with field data are recommended.

Effect of Pressure

Alhanati (1993) reported the effect of pressure on natural separation efficiency. According to Alhanati, the annulus efficiency decreases with increasing pressure.

Previous simplified models never incorporate the effects of pressure on the annulus efficiency. However, the model presented in this work considers this variable in the prediction and its effects on natural separation are shown in Fig. 14. According to this figure, pressure shows to have a strong effect on natural separation process. The bigger is the pressure, the smaller is the annulus efficiency. This fact corroborates the Alhanati's results obtained from experimental data.

Effect of Gas

Lea and Bearden (1980) conducted tests with 500 series equipment inside a 7" casing, with air and water as experimental fluids at low pressures (25 to 30 Psig). According to their results, natural separation efficiency increases as the in-situ-free gas increases. Alhanati and Sambangi also reported the same observation from their experimental work.

This work considers the effect of gas in the prediction on natural separation efficiency. The bubble size prediction considers how much gas is coming from the bottomhole. However, the gas effects predicted by this model are not strong as those observed in the experiments.

Conclusions and Recommendations

Some very important conclusions are summarized, as follows:

1. This paper presents a mechanistic model to predict natural separation efficiency. Based on drift-flux model, a new mathematical formulation was developed to estimate natural separation efficiency.
2. The new model considers the effect of slip velocity in the radial direction, a variable neglected in previous simplified models.
3. The new model is also a function of another important variables such as geometric characteristics of the bottomhole, gas and liquid flow rate.
4. Available experimental data was used to obtain a new correlation for the bubble drag radius, as a function of gas flow rate. Predictions of the model have been compared and verified against experimental data, shown good agreement.
5. The effect of pressure has been considered for this mechanistic model. Results show that the annulus efficiency decreases with increasing pressure, as reported for some authors.
6. The new approach takes into account the port size effect. However, additional real experimental data is required to further verify the results obtained by using the new model. In addition, the effect of fluid properties such as viscosity should be further considered as well.
7. Even though the solution of the mechanistic model requires a numerical method, the algebraic equations allow to adapt easily in any computational language.

Acknowledgement

Authors wish to thank TUALP member companies ENI-AGIP, CENTRILIFT, PEMEX, PDVSA-INTEVEP, ONGC, SCHLUMBERGER, SHELL AND TOTALFINALELF for supporting this study.

Nomenclature

A = Area, in^2
E = Natural Separation Efficiency
Q = Flow Rate, bpd
V = Velocity, ft/sec

Greek letters

ρ = Density, lbm/ft^3
σ = Surface Tension, lb/ft
g = Gravity, ft/sec^2
α = Void Fraction
∞ = Terminal

Subscripts

Ann = Annulus
g = Gas
i = Inlet
l = Liquid
p = Port, Pump
s = Slip, Superficial
r, z = Direction

References

1. Alhanati, F.J.S.: "Bottomhole Gas Separation Efficiency in Electrical Submersible Pump Installation", Dissertation. The University of Tulsa, 1993.
2. Ghauri, W.K.: "Production Technology Experience in a Large Carbonate Water-Flood, Denver Unit, Wasson San Andres Field, West Texas", paper SPE 8406 presented at the 1979 SPE Annual Technical Conference and Exhibition, Las Vegas, NV, Sep. 23-26.
3. Harmathy, T.Z., Velocity of Large Drops and Bubbles in Media of Infinite or Restricted Extent, *AIChE*, 6, 281(1960).
4. Harun, A.F., Prado, M.G., Serrano, J.C. and Doty, D.R.: "A Simple Model to Predict Natural Gas Separation Efficiency in Pumped Wells", paper SPE 63045 presented at the 2000 SPE Annual Technical Conference and Exhibition held in Dallas, Texas, 1-4 October 2000.

5. Ishii, M.: "Thermo Fluid Dynamic Theory of Two Phase Flow", Eyrolles, Paris, 1975.
6. Ishii, M. and Zuber, N.: "Drag Coefficient and Relative Velocity in Bubbly, Droplet or Particulate Fluids", *AIChE* Journal (September 1979) **25**, No. 5, 843-855.
7. Lea, J.F. "Effect of Gaseous Fluids on Submersible Pump Performance", paper SPE 9218 presented at the 1980 SPE Annual Technique Conference and Exhibition, Dallas, TX. (Sep. 21-24).
8. Marquez, R., "Classification of the experimental natural separation data according to flow pattern regime". Technical Report. The University of Tulsa, Tulsa, Ok. (2002).
9. Marquez, R.A. and Prado, M.G., "A new correlation for predicting natural separation efficiency". Southwestern Petroleum Short Course. April 16-17, 2003. Lubbock Memorial Civic Center, Lubbock, Texas.
10. Serrano, J.C.: "Natural Separation Efficiency in Electric Submersible Pump Systems", Dissertation. The University of Tulsa, 1999.
11. Wallis, G.B.: "The Terminal Speed of Single Drops or Bubbles in an Infinite Medium", *International Journal of Multiphase Flow* (1974) **1**, 491-511.
12. Zuber, N.: "On the Dispersed Two-Phase Flow in the Laminar Flow Regime", *Chem. Eng. Sci.*, 19, 897 (1964).

APPENDIX A
Algebraic Equation for the Superficial Gas Velocity Going into the Pump V_{rsg}^{p} and Gas Void Fraction α_g .

Based on a single control volume, as shown in Fig. 3, the following gas and liquid velocities field would be assumed valid in this work.

$$\overline{V}_{zg} = V_{zg}^{i} \;\; ; \;\; \overline{V}_{rg} = V_{rg}^{p} \qquad \text{(A-1)}$$

$$\overline{V}_{zl} = 0 \;\; ; \;\; \overline{V}_{rl} = V_{rl}^{p} \qquad \text{(A-2)}$$

On the other hand, slip velocity V_s is defined as:

$$V_s = \overline{V}_g - \overline{V}_l \qquad \text{(A-3)}$$

Where $\overline{V}_g$ and $\overline{V}_l$ represent the average actual gas and the liquid velocity, respectively.

Radial Direction

In the radial direction, slip velocity definition would be given by

$$V_{rs} = \overline{V}_{rg} - \overline{V}_{rl} \qquad \text{(A-4)}$$

According to the velocity field assumed for the gas and liquid phase, Eq. A-4 would be given by

$$V_{rs} = V_{rg}^{p} - V_{rl}^{p} \qquad \text{(A-5)}$$

V_{rg}^{p} and V_{rl}^{p} represent the average actual gas and liquid velocity, respectively. Using liquid hold up definition, Eq. A-5 can also be rewritten as a function of superficial velocity and gas void fraction as:

$$V_{rs} = \frac{V_{rsg}^{p}}{\alpha_g} - \frac{V_{rsl}^{p}}{(1-\alpha_g)} \qquad \text{(A-6)}$$

Assuming constant density, the following equation for V_{rsl}^{p} results valid

$$V_{rsl}^{p} = V_{zsl}^{i}\left(\frac{A_{Ann}}{A_p}\right) \qquad \text{(A-7)}$$

Therefore, the following equation for V_{rsg}^{p} can be obtained combining Eqs. A-6 and A-7.

$$V_{rsg}^{p} = \frac{\alpha_g}{1-\alpha_g}\left[V_{rs}\,(1-\alpha_g) + V_{zsl}^{i}\left(\frac{A_{Ann}}{A_p}\right)\right] \text{(A-8)}$$

Vertical Direction

Similarly, as in the radial direction, the slip velocity definition, given by Eq. A-3, can be used, obtaining the following result

$$V_{zs} = \overline{V}_{zg} = V_{zg}^{i} \qquad \text{(A-9)}$$

Rewritten Eq. A-9 as a function of superficial velocity and gas void fraction,

$$V_{zs} = \frac{V_{zsg}^{i}}{\alpha_g} \qquad \text{(A-10)}$$

Therefore, the following additional relationship for the gas void fraction can be obtained finally from Eq. A-10

$$\alpha_g = \frac{V_{zsg}^{i}}{V_{zs}} \qquad \text{(A-11)}$$

The solution of Eqs. A-8 and A-11 depends on two additional unknown variables: slip velocity in the radial and vertical direction, V_{rs} and V_{zs}, respectively.

Using the drfit-flux model approach proposed by Ishii (1975), the slip velocity V_s at any direction can be related to the terminal velocity of a bubble V_∞ and the gas void fraction, i.e.

$$V_s = V_\infty\,(1-\alpha_g)^{n-1} \qquad \text{(A-11)}$$

n represents the effect due to the presence of others bubbles. Some authors have considered that under slug/churn flow regime n can be neglected. Since most of the available experimental data is under this flow regime, then n was assumed equal to zero. Therefore, Eq. A-11 can be finally rewritten as

$$V_s = \frac{V_\infty}{(1-\alpha_g)} \qquad \text{(A-12)}$$

Eq. A-12 allows to rewritte Eqs. A-8 and A-11 as a function of the terminal velocity of the bubble, instead of slip velocity, in the radial and vertical direction.

$$V_{rsg}^{p} = \frac{\alpha_g}{1-\alpha_g}\left[V_{r\infty} + V_{zsl}^{i}\left(\frac{A_{Ann}}{A_p}\right)\right] \quad \text{(A-13)}$$

$$\frac{\alpha_g}{1-\alpha_g} = \frac{V_{zsg}^{i}}{V_{z\infty}} \quad \text{(A-14)}$$

APPENDIX B
Algebraic Equation for the Slip Velocity in the Vertical Direction.

Combining mass and momentum balance equations, given by Eqs. 7 and 9, the following system of equations can be defined

$$\begin{aligned} 0 &= -\alpha_g \frac{d}{dz}(P_g) - \alpha_g \rho_g g - M_g \\ 0 &= -\alpha_l \frac{d}{dz}(P_l) - \alpha_l \rho_l g + M_l \end{aligned} \quad \text{(B-1)}$$

Pressure gradient dP/dz and the interfacial drag term M represent the two unknown variables of this system. Solving this system of equations, dP/dz and M_g are given by

$$\frac{dP}{dz} = \rho_m g \quad \text{(B-2)}$$

$$M_g = \alpha_g (1-\alpha_g)(\rho_l - \rho_g) g \quad \text{(B-3)}$$

Where mixture density ρ_m is given by

$$\rho_m = \alpha_g \rho_g + \alpha_l \rho_l \quad \text{(B-4)}$$

By neglecting the lift force due to rotations of particles and the diffusion force due to the concentration gradient, the combined interfacial drag forces M_g acting on the dispersed phase may be modeled by a simple form proposed by Zuber (1964) as

$$\vec{M}_g = \frac{\alpha_g \vec{F}_g}{B_g} \quad \text{(B-5)}$$

Where B_g and α_g represent the volume of a single bubble and the gas void fraction, respectively. F_g represents the axial drag force for a single bubble, which is given by

$$F_g = -\frac{1}{2} C_d \rho_l V_{zs} \left|\vec{V}_s\right| A_d \quad \text{(B-6)}$$

A_d represents the projected area of a typical particle, V_{zs} the slip velocity at the vertical direction, and C_d the drag coefficient.

Therefore, the interfacial drag force M_g would be given by

$$M_g = \frac{\alpha_g \left(\frac{1}{2} C_d \rho_l V_{zs} \left|\vec{V}_s\right| A_g\right)}{B_g} \quad \text{(B-7)}$$

Because A_g can adopt any particular shape, the use of the following auxiliary definitions is recommended

Surface Area S_d

$$S_d = 4\pi r_d^2 \quad \text{(B-8)}$$

Sauter mean radius r_{sm}

$$r_{sm} = 3\frac{B_d}{S_d} \quad \text{(B-9)}$$

Drag radius r_d

$$r_d = \frac{3}{4}\frac{B_d}{A_d} \quad \text{(B-10)}$$

Particle density number N

$$N = \frac{\alpha_d}{B_d} \quad \text{(B-11)}$$

Interfacial area concentration a_i

$$a_i = N S_d \quad \text{(B-12)}$$

Using auxiliary definitions, Eq. B-7 can be rewritten as

$$M_g = \frac{1}{8}\frac{a_i r_{sm} C_d \rho_l}{r_d} V_{zs}\left|\vec{V}_s\right| \quad \text{(B-13)}$$

Combining Eqs. B-3 and B-13, the slip velocity in the vertical direction V_{zs} is given by

$$V_{zs} \frac{8 r_d}{a_i r_{sm} C_d \left|\vec{V}_s\right|} \alpha_g (1-\alpha_g) \frac{(\rho_l - \rho_g) g}{\rho_l} \quad \text{(B-14)}$$

APPENDIX C
Algebraic Equation for the Slip Velocity in the Radial Direction.

Combining mass and momentum balance equation given by Eqs. 7 and 8, the following system of equations can be obtained.

$$\begin{aligned} V_{rg}\frac{\partial}{\partial r}(\alpha_g \rho_g V_{rg}) &= -\alpha_g \frac{\partial}{\partial r}(P_g) - M_g \\ V_{rl}\frac{\partial}{\partial r}(\alpha_l \rho_l V_{rl}) &= -\alpha_l \frac{\partial}{\partial r}(P_l) + M_l \end{aligned} \quad \text{(C-1)}$$

Similar to vertical direction, dP/dz and M can be obtained by solving the system of equations. Assuming that $\rho_l >>> \rho_g$, the solution of that system would be given by

$$\frac{dP}{dr} = V_{rl}\frac{d}{dr}(\alpha_l \rho_l V_{rl}) \quad \text{(C-2)}$$

$$M_g = \alpha_g V_{rl}\frac{d}{dr}(\alpha_l \rho_l V_{rl}) \quad \text{(C-3)}$$

Using the interfacial drag definition in the radial direction, the following equation can be obtained

$$M_g = \frac{1}{8}\frac{a_i\, r_{sm}\, C_d\, \rho_l}{r_d} V_{rs} \left|\vec{V}_s\right| \qquad \text{(C-4)}$$

Combining Eqs. C-3 and C-4, the slip velocity in the radial direction V_{rs} would be given by

$$V_{rs} = \frac{8\, r_d}{a_i\, r_{sm}\, C_d \left|\vec{V}_s\right|} \alpha_g\,(1-\alpha_g)\left(V_{rl}\frac{d}{dr}(V_{rl})\right) \qquad \text{(C-5)}$$

TABLE 1. MODEL COMPARISONS

SIMPLIFIED MODEL	AVERAGE ERROR %	ABS. AVERAGE ERROR %	STANDARD DEVIATION %
SERRANO	-14.12	25.64	26.84
ALHANATI	-24.53	25.64	17.86
NEW CORRELATION	8.9	17.43	20.29
NEW MECHANISTIC MODEL	-7.97	15.24	16.97

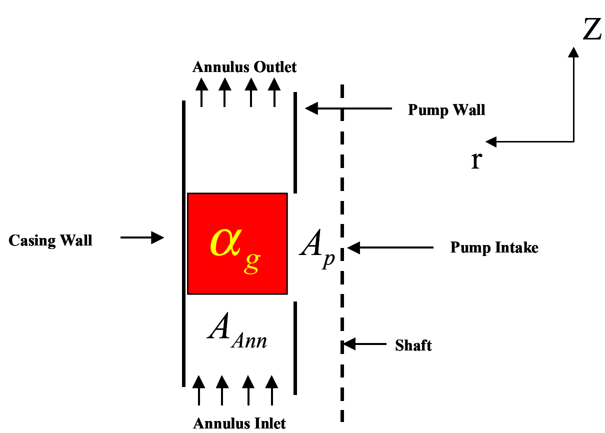

Figure 1. Single Cell Domain.

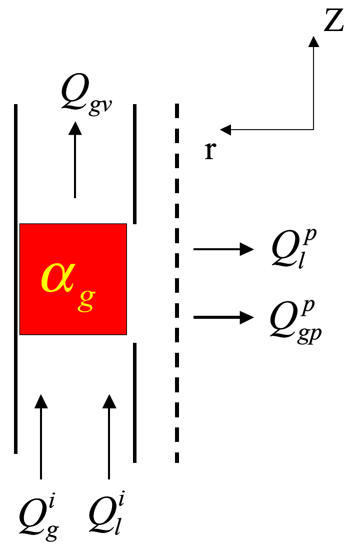

Figure 2. Volumteric Balance Around the Single Control Volume.

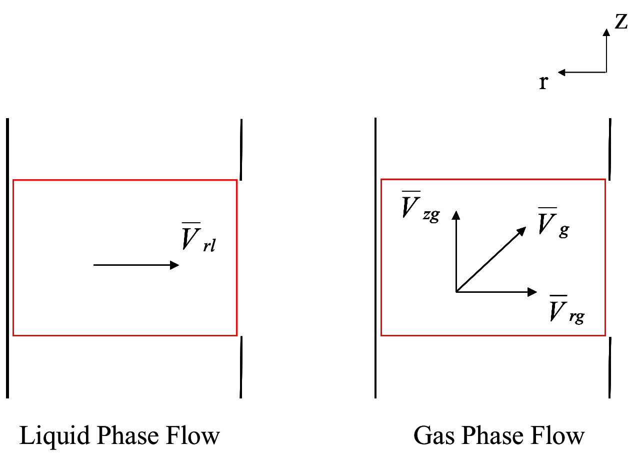

Figure 3. Velocities Field into the control volume. Gas and Liquid Phase flow.

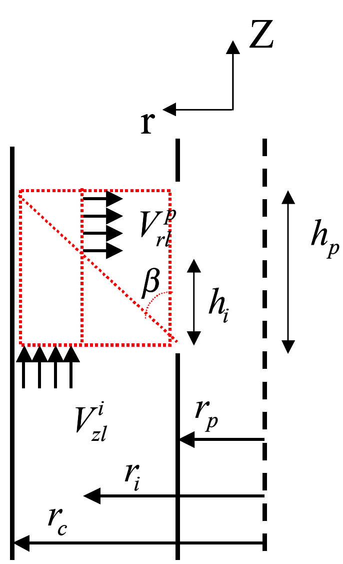

Figure 4. Sketch of a Single Cell Domain at Pump Intake

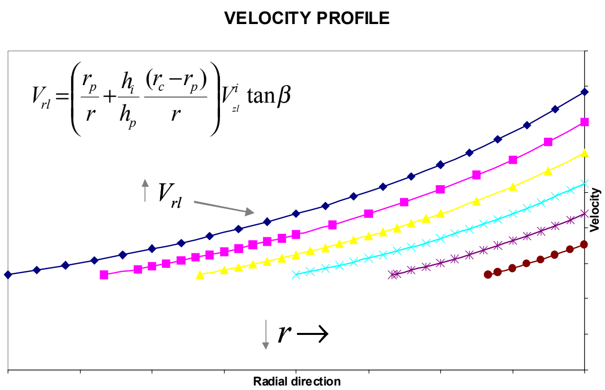

Figure 5. Liquid phase Velocity Profile.

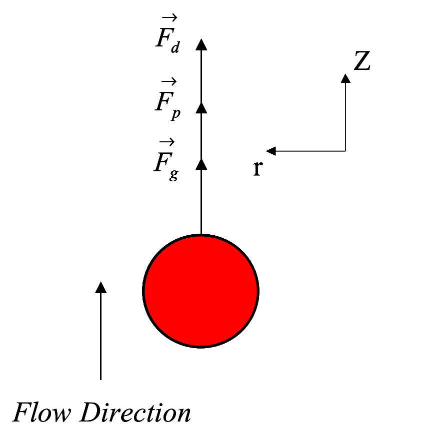

Figure 6. Free-Body Diagram - Vertical Direction

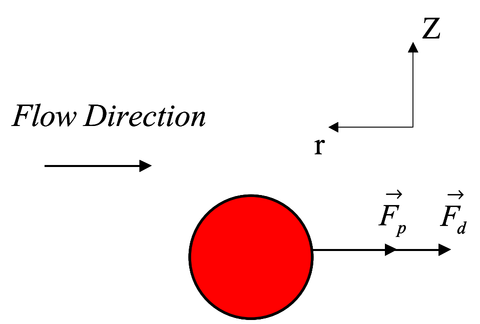

Figure 7. Free-Body Diagram - Horizontal Direction

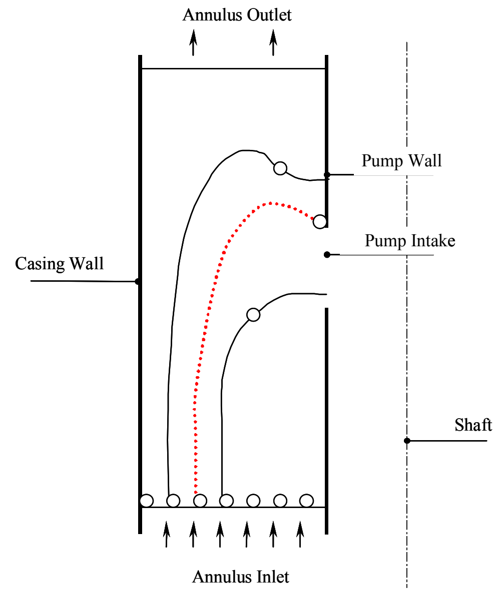

Figure 8. Trajectory of the Bubbles into the Flow Domain.

$$E = \frac{r_c^2 - r_s^2}{r_c^2 - r_p^2}$$

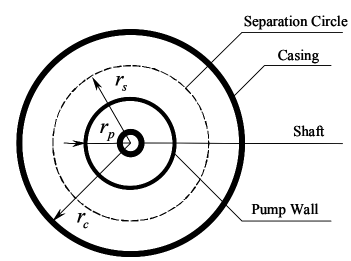

Figure 9. Cross-section of the well bore.

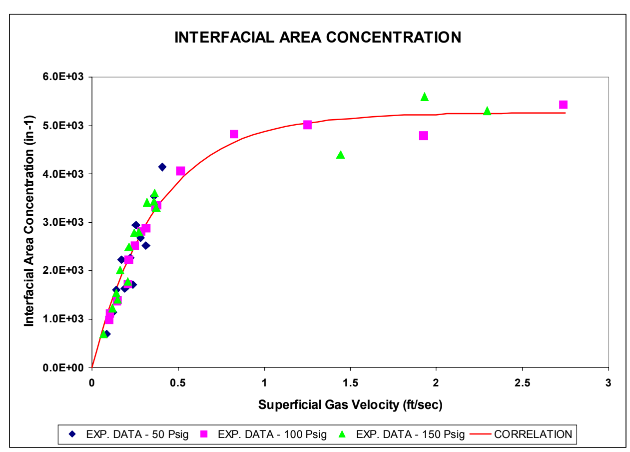

Figure 10. Correlation for Interfacial Area Concentration a_i.

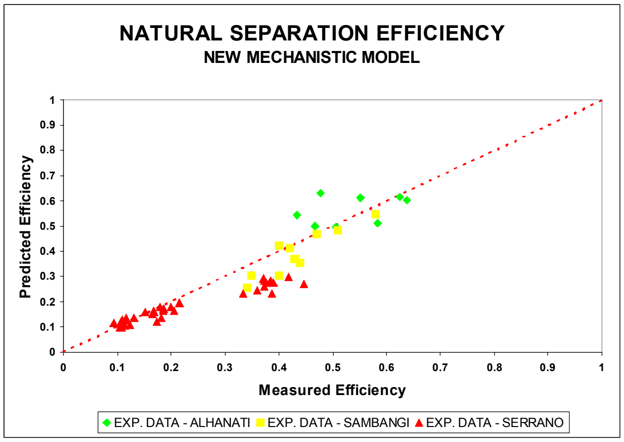

Figure 11. Measured and Predicted Efficiency. Natural Separation Efficiency.

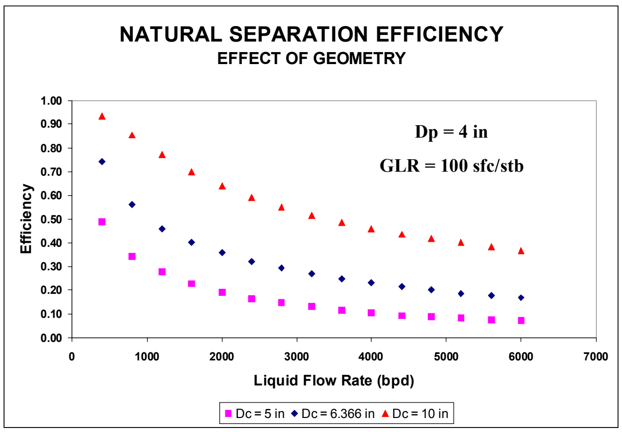

Figure 12. Effect of Annulus Size on Natural Separation Efficiency.

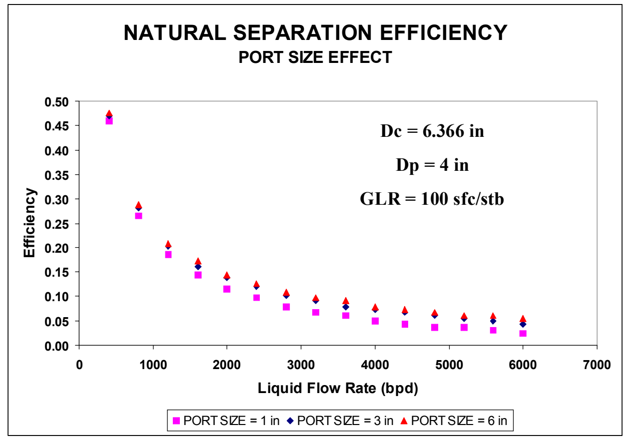

Figure 13. Effect of Port Size on Natural Separation Efficiency.

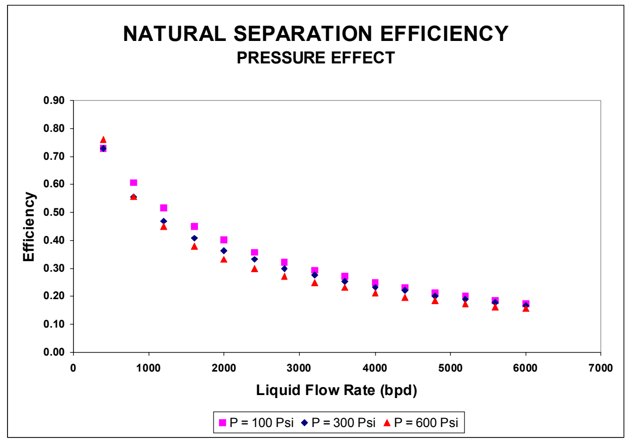

Figure 14. Effect of Pressure on Natural Separation Efficiency.